AIAA JOURNAL
Vol. 42, No. 8, August 2004

Uncertainty Propagation for a Turbulent, Compressible Nozzle Flow Using Stochastic Methods

Lionel Mathelin* and M. Yousuff Hussaini†
Florida State University, Tallahassee, Florida 32306-4120
Thomas A. Zang‡
NASA Langley Research Center, Hampton, Virginia 23681-2199
and
Françoise Bataille§
Centre de Thermique de Lyon, 69621 Villeurbanne, France

A fully spectral, polynomial chaos method for the propagation of uncertainty in numerical simulations of compressible, turbulent flow is described. The method is applied to the flow in a quasi-one-dimensional nozzle. Results demonstrate the ability of the method to propagate accurately the uncertainty throughout the entire numerical field. Comparison and validation were made with the reference Monte Carlo method. An exact method and an approximate method for the computation of inner products are also discussed in terms of efficiency and number of operations required.

Introduction

AN admittedly small but nevertheless noticeably accelerating trend within the computational fluid dynamics (CFD) community is changing the vision of computational aerodynamics from one of producing a solution as accurately as possible to one of producing a solution with acceptable uncertainty bounds. Most of the effort of the traditional CFD community has been focused on discretization error and turbulence modeling error. Some of the early advocates of a broader perspective on CFD uncertainty were Mehta,[1] Roache,[2] Coleman and Stern,[3] and Oberkampf and Blottner.[4] In the past half-dozen years, there have been several events that have served to increase awareness of the broader perspective on CFD uncertainty: 1) the publication of the AIAA guidelines on the verification and validation for CFD,[5] 2) the Drag Prediction Workshop sponsored by the AIAA Applied Aerodynamics Technical Committee,[6] and 3) the pair of sessions on CFD uncertainty at the January 2003 AIAA Aerospace Sciences Meeting.[7–19] (Links to all of the presentations at the Drag Prediction workshop are available at URL: http://ad-www.larc.nasa.gov/tsab/cfdlarc/aiaa-dpw/.) The work of Oberkampf et al.[20] and Oberkampf and Trucano[21] is especially notable for proposing a framework for characterization of uncertainties. Walters and Huyse[22] have provided a tutorial on uncertainty methods aimed at a CFD audience. Luckring et al.[10] have presented a comprehensive vision for approaching computational aerodynamics uncertainty. (Their choice of title is noteworthy in that their vision is not confined to Euler and Navier–Stokes methods but embraces the use of simpler aerodynamic models.) Zang et al.[23] have outlined the needs and opportunities for uncertainty quantification and optimization under uncertainty research for aerospace applications.

Some, but by no means all, of the uncertainties affecting CFD are reasonably described in probabilistic terms. (See Oberkampf et al.[24] for a general mathematical framework for describing uncertainties.) Our focus in this work is on stochastic methods for quantifying those uncertainties which can be described by probability density functions (PDFs). A fundamental task for these methods is to propagate prescribed uncertainty distributions on the input parameters, for example, boundary conditions, or code parameters, for example, turbulence modeling coefficients, through the CFD code to the output field variables and ultimately to the relevant output functionals of the simulation. Standard sampling techniques, such as Monte Carlo, are exact methods for accounting for this type of uncertainty quantification in the sense that they do not require any approximations of the CFD analysis nor any assumptions on the input PDFs. Moreover, sampling techniques provide the full set of output statistics, albeit with obvious limitations on accuracy related to the number of samples. However, standard Monte Carlo is clearly intractable for large CFD problems because it easily requires thousands of simulations for meaningful results. Although more sophisticated sampling techniques such as importance sampling and Latin hypercube sampling are well established, we are unaware of any attempts yet to use these for CFD applications. Cao et al.[25] have recently presented a nonstandard variance reduction technique that exploits sensitivity derivatives. They demonstrated that it reduces the sampling requirements by at least one order of magnitude on an aircraft wing structural application. This approach seems ideally suited to CFD applications with a large number of input uncertainty variables provided that the CFD code can produce efficient sensitivity derivatives.

The moment methods are an efficient approximate approach. They involve expanding the variables of the problem in terms of Taylor series around their mean value (see Ref. 26). This technique allows for a quick estimation of the low-order statistics but requires at a minimum an efficient procedure for computing first-order sensitivity derivatives.

In this paper, we explore the use of a stochastic PDE approach, that is, adding one or more stochastic variables to the deterministic CFD equations, as an alternative to sampling techniques.

Le Maître et al.,[27,28] Xiu et al.,[29] and Xiu and Karniadakis[30,31] pioneered the stochastic PDE approach to uncertainty quantification for CFD. Both approaches are based on the homogeneous chaos expansions introduced by Wiener[32] and extended and applied extensively by Ghanem and Spanos[33] and Ghanem[34] for stochastic

Presented as Paper 2003-4240 at the AIAA 16th Computational Fluid Dynamics Conference, Orlando, FL, 23–26 June 2003; received 8 October 2003; revision received 17 February 2004; accepted for publication 17 March 2004.

*Research Associate, School of Computational Science and Information Technology; currently Research Associate, Laboratoire d'Informatique pour la Mécanique et les Sciences de l'Ingénieur–Centre National de la Recherche Scientifique, B.P. 133, 91403 Orsay Cedex, France.

†Professor, School of Computational Science and Information Technology.

‡Senior Technologist, Aerospace Systems, Concepts and Analysis Competency. Associate Fellow AIAA.

§Professor, Institut National des Sciences Appliquées.

PDE solutions to structural problems. Xiu and Karniadakis[30] extended this polynomial chaos (PC) expansion method to a wide variety of basis functions for the stochastic component. Le Maître et al.[27,28] applied the PC concept to a microchannel and cavity flow, whereas Debusschere et al. used it to quantify the uncertainty of protein labeling reactions.[35] Xiu and Karniadakis[31] demonstrated the PC method to incompressible flow in a channel and flow past a circular cylinder. Walters and Huyse[22] include PC examples in their tutorial, and Walters[14] has explained how to deal correctly with the grid movement terms necessary to compute the effects of geometric uncertainties in PC applications. Our contribution here is the extension of the CFD PC approach to include a two-equation turbulence model. The demonstration of the method is given for a quasi-one-dimensional nozzle flow.

Stochastic PDE Fundamentals

The basic idea of the PC approach is to project the random variables of the problem onto a stochastic space spanned by a set of complete orthogonal polynomials Ψ that are functions of a random variable $\xi(\theta)$, where θ is a random event. The terms of the polynomial are functions of $\xi(\theta)$ and are, thus, functionals. Many types of random variables can be used: For example, $\xi(\theta)$ can be a Gaussian variable associated with Hermite polynomials. See Dunford and Schwartz[36] for more background on this theory.

More specifically, let u be a random variable defined as a mapping from a probability space $\mathcal{P}$ into $\mathbb{R}$. The probability space is defined by $\mathcal{P} = (\Omega; \Theta; \mu)$ with Ω the set of events, Θ a σ algebra, and μ the probability measure.

The original form of PC was restricted to expansions in Hermite polynomials. Xiu and Karniadakis[30] applied this concept to expansions in terms of Askey polynomials, for example, Laguerre polynomials for random variables with a Gamma distribution, and Jacobi polynomials for beta distributions. Obviously, the convergence rate, and, thus, the number of terms in the expansion required for a given accuracy, depends both on the random process to be approximated and on the choice of expansion functions.

We confine ourselves to Hermite expansions in the present work. Cameron and Martin[37] have shown that this expansion converges to any L_2 functionnal in the L_2 sense. Thus, it provides a mean to express a second-order random process, that is, with a finite second-order moment. When this approach is used, each dependent variable of the problem is expanded as, for example, for the velocity u,

$$u(\boldsymbol{x}, t, \theta) = \sum_{i=0}^{\infty} u_i(\boldsymbol{x}, t)\Psi_i[\xi(\theta)] \tag{1}$$

For practical simulations, the series has to be truncated to a finite number of terms, hereafter denoted N_{PC}. This framework remains valid also for multiple random variables, including uncorrelated or partially correlated random variables. In that case, the dependent variables of the problem are functions of several independent random variables and $\boldsymbol{\xi}$ is now a vector. The expression for the multidimensional Hermite polynomial or order n, H_n, is

$$H_n\left(\xi_{i_1}, \ldots, \xi_{i_n}\right) = (-1)^n e^{\frac{1}{2}\xi^T\xi} \frac{\partial^n}{\partial\xi_{i_1}\ldots\partial\xi_{i_n}} e^{-\frac{1}{2}\xi^T\xi} \tag{2}$$

As discussed by Ghanem and Spanos,[33] there is a one-to-one correspondence between $H_n(\boldsymbol{\xi})$ and $\Psi_i(\boldsymbol{\xi})$. The general expression for the PC is given by

$$u(\boldsymbol{x}, t, \theta) = \sum_{i=0}^{N_{\mathrm{PC}}} u_i(\boldsymbol{x}, t)\Psi_i[\boldsymbol{\xi}(\theta)] \tag{3}$$

with the number of terms N_{PC} determined from

$$N_{\mathrm{PC}} + 1 = \frac{(n_{\mathrm{pc}} + p_{\mathrm{pc}})!}{n_{\mathrm{pc}}!\, p_{\mathrm{pc}}!} \tag{4}$$

where p_{pc} is the order of the expansion and n_{pc} the dimensionality of the chaos, that is, the number of independent random variables. (Note that the dimensionality of the chaos is not the same as the number of physical dimensions of the problem.) It follows that N_{PC} grows very quickly with the dimension of the chaos and the order of the expansion.

In the case of the Hermite polynomials, the zeroth-order term represents the mean value and the first-order term the Gaussian part, whereas higher orders account for non-Gaussian contributions. Spectral coefficients are determined using a Galerkin projection onto the stochastic basis. This inner product in the stochastic space is expressed as

$$\langle f_1(\boldsymbol{\xi}) f_2(\boldsymbol{\xi})\rangle = \int_{-\infty}^{\infty} f_1(\boldsymbol{\xi}) f_2(\boldsymbol{\xi}) w(\boldsymbol{\xi})\, \mathrm{d}\boldsymbol{\xi} \tag{5}$$

where the weight function $w(\boldsymbol{\xi})$ is the n_{pc}-dimensional normal distribution

$$w(\boldsymbol{\xi}) = \left[1\Big/\sqrt{(2\pi)^{n_{\mathrm{pc}}}}\right] e^{-\frac{1}{2}\xi^T\xi} \tag{6}$$

In the L_2 norm, we, thus, get

$$\langle \Psi_i \Psi_j\rangle = \left\langle \Psi_i^2 \right\rangle \delta_{ij} \tag{7}$$

where δ is the Kronecker operator. The statistics of any order for a variable or set of variables can be determined from their PC expansions.[30]

Let us consider now the task of computing the PC expansion of the product of two random variables a and b, which are given as PC expansions with N_{PC} terms. The Galerkin projection scheme yields for the expansion coefficients of the product ab:

$$(ab)_k = \sum_{i=0}^{N_{\mathrm{PC}}} \sum_{j=0}^{N_{\mathrm{PC}}} a_i b_j \langle \Psi_i \Psi_j \Psi_k\rangle, \qquad \forall k \in [0; N_{\mathrm{PC}}] \subset \mathbb{N} \tag{8}$$

When it is assumed that the terms $\langle \Psi_i \Psi_j \Psi_k\rangle$ have been precomputed and stored, the evaluation of the sum (8) takes $3(N_{\mathrm{PC}}+1)^3$ operations (two multiplications and one addition for each term in the sum). The complexity becomes even greater for higher-order products. In particular, to compute the expansion coefficients of a Qth-order product takes $3(N_{\mathrm{PC}}+1)^{Q+1}$ operations.

An alternative approach is to resort to numerical quadrature in lieu of the analytical summation used in the Galerkin projection. The inner product (5) may then be approximated by

$$\langle f_1(\boldsymbol{\xi}) f_2(\boldsymbol{\xi})\rangle \simeq \sum_{l=1}^{M} f_1(\boldsymbol{\xi}_l) f_2(\boldsymbol{\xi}_l) w(\boldsymbol{\xi}_l) \tag{9}$$

where M is the number of Gauss–Hermite quadrature points that are utilized. Such a quadrature rule is exact for all polynomials of degree $2M$ or less.

The quadrature-based evaluation of the coefficients for the ab product is now expressed as

$$(ab)_k \simeq \sum_{l=1}^{M} \left\{ \left[\sum_{i=0}^{N_{\mathrm{PC}}} a_i \Psi_i(\boldsymbol{\xi}_l) \right] \left[\sum_{i=0}^{N_{\mathrm{PC}}} b_i \Psi_i(\boldsymbol{\xi}_l) \right] \Psi_k(\boldsymbol{\xi}_l) w(\boldsymbol{\xi}_l) \right\}$$

$$\forall k \in [0; N_{\mathrm{PC}}] \subset \mathbb{N} \tag{10}$$

where $\boldsymbol{\xi}$ is now assumed to be a scalar (one stochastic dimension) and in the present case the integrand is a polynomial of degree $3N_{\mathrm{PC}}$ or less. Therefore, taking $M \geq \frac{3}{2}N_{\mathrm{PC}}$ produces an exact evaluation of the PC coefficients of the product ab.

Computing the N_{PC} coefficients via sum (10) requires $4M(N_{\mathrm{PC}}+1)(N_{\mathrm{PC}}+2)$ operations. More generally, let us denote by Q the dimensionality of the nonlinear term that is to be evaluated. To leading order, the Galerkin approach takes $3(N_{\mathrm{PC}}+1)^{Q+1}$ operations, whereas the quadrature approach takes $2QM(N_{\mathrm{PC}}+1)^2$ operations. Using the quadrature approach with $M = [(Q+1)/2]N_{\mathrm{PC}}$

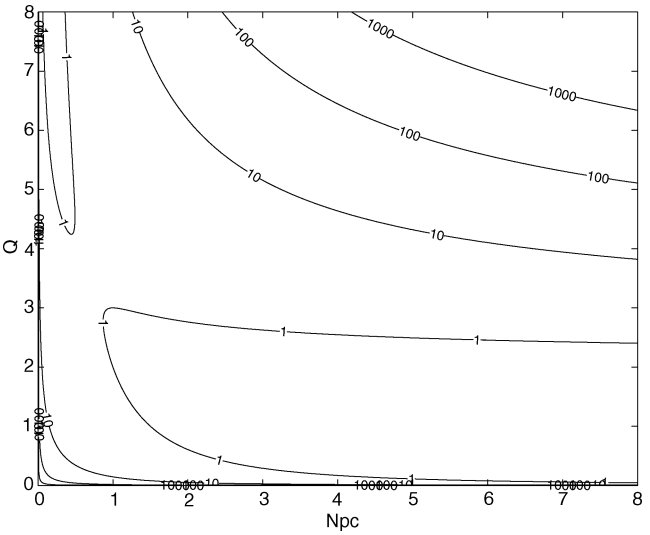

Fig. 1 Isocontours of the relative cost of the exact over the quadrature rule for a Q-dimensional product of N_{PC}th order.

yields the exact solution to the expansion coefficients of the Qth-order product in order $Q(Q+1)N_{\mathrm{PC}}(N_{\mathrm{PC}}+1)^2$ operations. Of course, one could also just use $M = N_{\mathrm{PC}}$ at the cost of errors in the quadrature rule.

Figure 1 shows the relative cost of the exact method compared to the quadrature rule as a function of the nonlinearity of the problem Q and the order of PC expansion N_{PC}.

In the case of a second-order, two-dimensional PC expansion as considered in this paper, we have $N_{\mathrm{PC}} = 5$, and according to the result from Fig. 1, the quadrature method requires fewer operations than the exact method for nonlinear terms of order higher than two. More generally, the higher the nonlinearity order and/or the number of terms retained in the PC expansion, the faster the quadrature method is compared to the exact method. The quadrature method is, thus, most appropriate for highly nonlinear equations with a relatively large number of independent random variables.

Here, the most complex (and slowest to compute) terms are involved in the ϵ equation and lead to $Q = 7$ (see the Appendix). Because the CPU time requirement is not an issue in the current paper, the more exact integral expression was used for the stochastic inner products throughout the study.

In the next section, we furnish the governing equations and uncertainty description for a quasi-one-dimensional nozzle. The subsequent section covers the discretization procedures. The fifth section presents representative results for quasi-one-dimensional nozzle flow using PC.

Stochastic Quasi-One-Dimensional Nozzle Flow

As a first step in evaluating the stochastic PDE approach to uncertainty quantification for compressible, turbulent flow, the PC technique is applied to a quasi-one-dimensional nozzle flow. The physics of the phenomena involved in a nozzle flow are well understood, and the configuration is simple enough to allow focusing on the stochastic treatment rather than on numerical problems, making this configuration an appropriate choice. Mathelin and Hussaini[38] presented initial results for inviscid quasi-one-dimensional nozzle flow using PC, and Mathelin et al.[39] presented a more extensive discussion of the inviscid flow application. Here, we add both viscosity and a two-equation turbulence model to explore the issues in extending this methodology to the full three-dimensional, compressible, Reynolds-averaged Navier–Stokes equations.

Laminar Equations

The equations for laminar, viscous, quasi-one-dimensional nozzle flow in conservative form are

$$\boldsymbol{Q}_t + \boldsymbol{F}_x = \boldsymbol{S} \tag{11}$$

where

$$\boldsymbol{Q} = \begin{bmatrix} \rho A \\ \rho u A \\ \rho E A \end{bmatrix}$$

$$\boldsymbol{F} = \begin{bmatrix} \rho u A \\ \dfrac{3-\gamma}{2}\rho u^2 A + (\gamma-1)\rho E A - \left(\dfrac{4}{3}\mu\right) A \dfrac{\partial u}{\partial x} \\ \gamma \rho u E A - \dfrac{\gamma-1}{2}\rho u^3 A - \dfrac{(\gamma-1)\bar{M}}{R}(\lambda) A \dfrac{\partial}{\partial x}\left(E - \dfrac{u^2}{2}\right) \end{bmatrix}$$

$$\boldsymbol{S} = \begin{bmatrix} 0 \\ (\gamma-1)\left[\rho E - \dfrac{\rho u^2}{2}\right]\dfrac{\partial A}{\partial x} \\ 0 \end{bmatrix} \tag{12}$$

where ρ is the density, u the velocity, A the nozzle cross-section area, E the total energy, γ the specific heat ratio ($\gamma = 1.4$ for diatomic gas), μ the laminar dynamic viscosity, λ the laminar thermal diffusivity, R the ideal gas constant, and $\bar{M}$ the fluid molar mass. The static pressure P has been removed from the equations by making use of

$$E = [P/(\gamma-1)\rho] + \tfrac{1}{2}u^2 \tag{13}$$

Turbulence Equations

The turbulence model considered here is the standard two-equation k–ϵ model. The reasons for that choice are that considering the geometry and the quasi-one-dimensional assumption, there is no need for a sophisticated turbulence model. Meanwhile, the k–ϵ model has features that also allow us to study the impact of uncertainty in the model coefficients (C_μ, C_{ϵ_1}, and C_{ϵ_2}) on the simulated field behavior and characteristics.

The second and third components of $\boldsymbol{F}$ in Eq. (12) are modified by replacing the $(\frac{4}{3}\mu)$ term by

$$\left(\tfrac{4}{3}\mu + 2\rho\nu_t\right) \tag{14}$$

and the term λ by

$$[\lambda + \rho(\nu_t/Pr_t)] \tag{15}$$

respectively, where ν_t is the turbulent kinematic viscosity and the turbulent Prandtl number $Pr_t = \mu_t/\lambda_t$ is assumed constant.

To these must be added the k–ϵ model equations, which reduce to

$$\frac{\partial}{\partial x}(\rho u k A) = \frac{\partial}{\partial x}\left[\rho A\left(\nu + \frac{\nu_t}{\sigma_k}\right)\frac{\partial k}{\partial x}\right] + 2\rho\nu_t A\left(\frac{\partial u}{\partial x}\right)^2 - \rho\epsilon A$$

$$\frac{\partial}{\partial x}(\rho u \epsilon A) = \frac{\partial}{\partial x}\left[\rho A\left(\nu + \frac{\nu_t}{\sigma_\epsilon}\right)\frac{\partial \epsilon}{\partial x_j}\right] + 2C_{\epsilon_1}\frac{\epsilon}{k}\rho\nu_t A\left(\frac{\partial u}{\partial x}\right)^2 - C_{\epsilon_2}\rho\frac{\epsilon^2}{k}A \tag{16}$$

for the steady state. Here, k is the turbulent kinetic energy, and ϵ is the turbulent dissipation rate. The turbulent viscosity coefficient is defined by

$$\nu_t = C_\mu(k^2/\epsilon) \tag{17}$$

The standard values of the turbulence model coefficients are $C_{\epsilon_1} = 1.44$, $C_{\epsilon_2} = 1.92$, $C_\mu = 0.09$, $\sigma_k = 1.0$, and $\sigma_\epsilon = 1.3$.

Nozzle Geometry Uncertainty Description

One source of uncertainty is in the nozzle shape, due to unavoidable manufacturing variability. Let $A(x)$ be Gaussian and partially correlated along the x direction following the autocorrelation function given by

$$C_{AA}(x_1, x_2) = \sigma_A^2 \exp(-|x_1 - x_2|/b) \tag{18}$$

where b is the correlation length and σ_A^2 the associated variance. The Karhunen–Loeve decomposition is used to represent this first-order Markovian process in the standard manner. Indeed, when the structure of the covariance function C_{AA} is known and characterized, the Karhunen–Loeve decomposition is the most effective representation of the random process. The Karhunen–Loeve expansion relies on the decomposition of the process onto a basis spanned by its eigenfunctions. Specifically, C_{AA} can be represented by

$$C_{AA}(x_1, x_2) = \sum_{i=0}^{\infty} \lambda_i f_i(x_1) f_i(x_2) \tag{19}$$

where λ_i are the eigenvalues and f_i the eigenfunctions of the covariance kernel determined from the eigenvalues problem

$$\int_{\Omega_A} C_{AA}(x_1, x_2) f_i(x_2)\, \mathrm{d}x_2 = \lambda_i f_i(x_1) \tag{20}$$

A can, thus, be expressed as

$$A(x) = \bar{u} + \sum_{i=1}^{\infty} \xi_i(\theta) \sqrt{\lambda_i} f_i(x) \tag{21}$$

See Ghanem and Spanos[33] for more details on the Karhunen–Loeve expansion for this particular problem.

Test Problem

The problem studied here is that of a supersonic diverging nozzle, as shown in Fig. 2. The inflow conditions are a Mach number of 1.2, a 1-atm static pressure, and unit density. The nozzle starts at $x = 0.3$ m and ends at $x = 5.5$ m. Uncertainty is considered to arise from nozzle geometry, inlet boundary conditions (pressure, velocity, and density), and turbulence model coefficients. Here, we consider $b = 20$ m and $\sigma_A = 0.05$ m^2 as describing the nozzle variability in Eq. (18). Because of the rapid decay of the eigenvalues of the Karhunen–Loeve expansion for this set of parameters, only the first two eigenfunctions are retained in the expansion that describes the nozzle geometry uncertainty. The resulting fuzzy cross section area is plotted in Fig. 3.

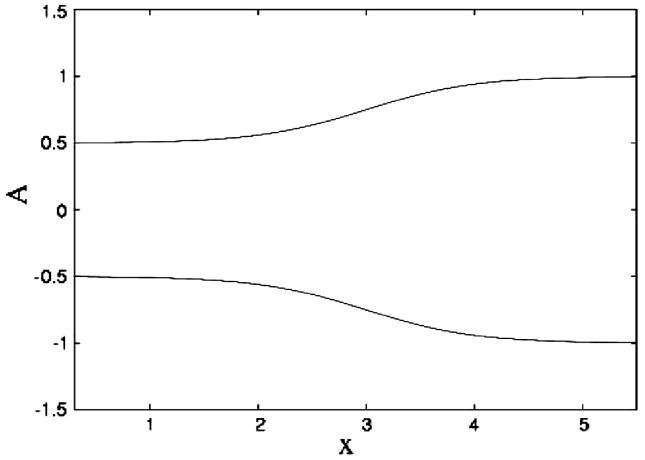

Fig. 2 Nozzle cross-sectional shape along the streamwise distance x; flow from left to right.

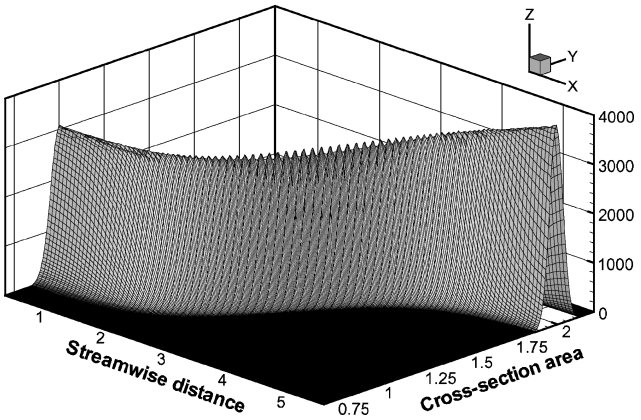

Fig. 3 Stochastic cross-sectional area PDF along the nozzle; PDF not normalized.

For turbulent flow, the additional inflow conditions are $k = 253$ m$^2 \cdot$ s^{-2} (5% turbulence intensity) and $\epsilon = 11{,}500$ m$^2 \cdot$ s^{-3}. The mean value (from the turbulence point of view) results for turbulent flow are indistinguishable graphically from those for the inviscid flow.

Discretization

Physical Space

The quasi-one-dimensional equations are discretized using the spectral element method combined with a fourth-order Runge–Kutta scheme in time. This spatial discretization is consistent with the spectral expansion involved in the PC technique.

For simplicity, we will discuss only the inviscid problem in detail. The laminar version of Eq. (12) is projected onto a spectral and stochastic basis and the Galerkin technique is applied. The spectral space is spanned by Chebyshev polynomials on the nodal points (in local coordinates $\bar{x} \in [-1; 1]$):

$$\bar{x}_n = \cos(\pi n/N), \qquad \forall n \in [0; N] \subset \mathbb{N} \tag{22}$$

where N is the number of points within each element.

The interpolants of variables, for example, u, in spectral space read as

$$u(\bar{x}, t) = \sum_{n=0}^{N} u_n(t) h_n(\bar{x}) \tag{23}$$

where

$$h_n(\bar{x}) = \frac{2}{N} \sum_{m=0}^{N} \frac{1}{\bar{c}_n \bar{c}_m} T_m(\bar{x}_n) T_m(\bar{x}) \tag{24}$$

with T_m the Chebyshev polynomials and $\bar{c}_i$ such as

$$\bar{c}_i = 2, \qquad i \in \{0; N\} \subset \mathbb{N} \tag{25}$$

$$\bar{c}_i = 1, \qquad i \in]0; N[\subset \mathbb{N} \tag{26}$$

Polynomial Chaos

Similarly, in the stochastic space,

$$u(x, t, \theta) = \sum_{i=0}^{N_{\mathrm{PC}}} u_i(x, t) \Psi_i[\xi(\theta)] \tag{27}$$

The following equation for the flux component of the momentum equation illustrates the computational complexity of the

discretization for just the inviscid problem:

$$\frac{\partial F_2}{\partial x} = \sum_{i=0}^{N_{PC}}\sum_{j=0}^{N_{PC}}\sum_{k=0}^{N_{PC}}\sum_{r=0}^{N_{PC}}\sum_{n=0}^{N}\sum_{m=0}^{N}\sum_{o=0}^{N}$$
$$\frac{3-\gamma}{2}\rho_{i,n}u_{j,m}u_{k,o}\langle\Psi_i\Psi_j\Psi_k\Psi_r\Psi_l\rangle$$
$$\times\left\{(h_n,h_m,h_o,h_p)\frac{\partial A_k}{\partial x}A_k\left[\left(\frac{\partial h_n}{\partial x},h_m,h_o,h_p\right)\right.\right.$$
$$\left.\left.+\left(h_n,\frac{\partial h_m}{\partial x},h_o,h_p\right)+\left(h_n,h_m,\frac{\partial h_o}{\partial x},h_p\right)\right]\right\}$$
$$+(\gamma-1)\sum_{i=0}^{N_{PC}}\sum_{j=0}^{N_{PC}}\sum_{k=0}^{N_{PC}}\sum_{n=0}^{N}\sum_{m=0}^{N}\rho_{i,n}E_{j,m}$$
$$\times\langle\Psi_i\Psi_j\Psi_k\Psi_l\rangle\left\{(h_n,h_m,h_p)\frac{\partial A_k}{\partial x}\right.$$
$$\left.+A_k\left[\left(\frac{\partial h_n}{\partial x},h_m,h_p\right)+\left(h_n,\frac{\partial h_m}{\partial x},h_p\right)\right]\right\} \quad (28)$$

The scalar products in the spectral space are defined by, for example, for (h_n, h_m, h_o),

$$(h_n,h_m,h_o)=\int_{-1}^{1}h_n(\bar{x})h_m(\bar{x})h_o(\bar{x})\,\mathrm{d}\bar{x}$$
$$=\frac{8}{N^3}\sum_{a=0}^{N}\sum_{b=0}^{N}\sum_{c=0}^{N}\frac{T_a(\bar{x}_n)T_b(\bar{x}_m)T_c(\bar{x}_o)}{\bar{c}_a\bar{c}_b\bar{c}_c\bar{c}_n\bar{c}_m\bar{c}_o}$$
$$\times\int_{-1}^{1}T_a(\bar{x})T_b(\bar{x})T_c(\bar{x})\,\mathrm{d}\bar{x} \quad (29)$$

In the stochastic space, we have for a two-dimensional PC, for example $\langle\Psi_i\Psi_j\Psi_k\Psi_l\rangle$,

$$\langle\Psi_i\Psi_j\Psi_k\Psi_l\rangle=\frac{1}{\sqrt{(2\pi)^2}}\int_{-\infty}^{\infty}\int_{-\infty}^{\infty}\Psi_i\Psi_j\Psi_k\Psi_l e^{-\frac{1}{2}\xi^T\xi}\,\mathrm{d}\boldsymbol{\xi}$$

The full equations for the inviscid problem are available in Ref. 40. The nonlinearity in the inviscid momentum flux results in a seven-dimensional summation in Eq. (28). Four of these sums are due to the PC expansion and would remain even for a simple finite difference spatial discretization.

The equations for the turbulence quantities ν_t, k, and ϵ are given in the Appendix in Eqs. (A3–A5).

Sample Results

Deterministic Part

The equations were first solved deterministically for verification of the numerical accuracy of the deterministic part of the code. The distribution along the nozzle of the mean values of the dependent variables, normalized with respect to their inlet value, is plotted in Fig. 4. The flow is from left to right. As the fluid flows along the diverging nozzle, the pressure and density decrease while the velocity and total energy increase. This behavior is fully consistent with the expected evolution of supersonic diverging flows. Computations were made with 61 points along the nozzle (30 elements with 3 points per element). Tests were conducted increasing the number of both the elements and the points per element up to a total of 321 (80 elements with 5 points per element). No appreciable difference was found, and the coarse grid was, thus, retained for CPU time economy.

Because this paper is not intended to provide any quantitative results, no further test was conducted into the deterministic part.

PC Validation

The PC approach was first compared to Monte Carlo (MC) simulations for the inviscid problem. The method used here is the regular MC method and does not take advantage of any accelerating technique. All of the inlet conditions are set Gaussian and fully correlated. The cross-sectional area is here assumed deterministic. MC simulations are carried with over 9 million independent samples, whereas the PC is one-dimensional, second order, that is, there is one independent random variable and second-order Hermite polynomial expansions are used.

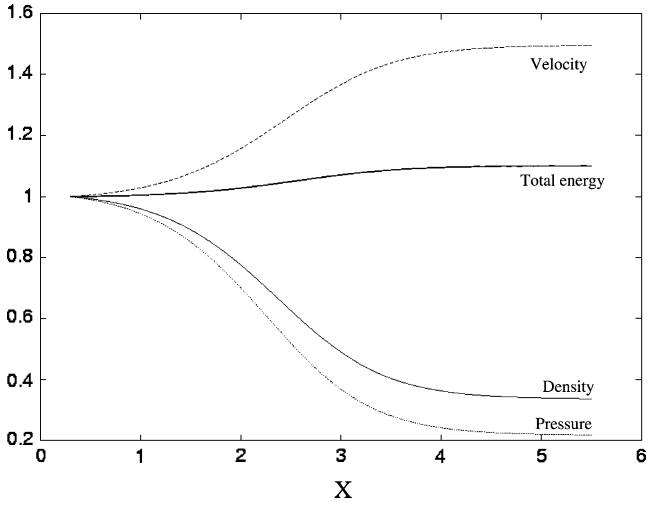

Fig. 4 Normalized flow variables mean value distribution along the nozzle.

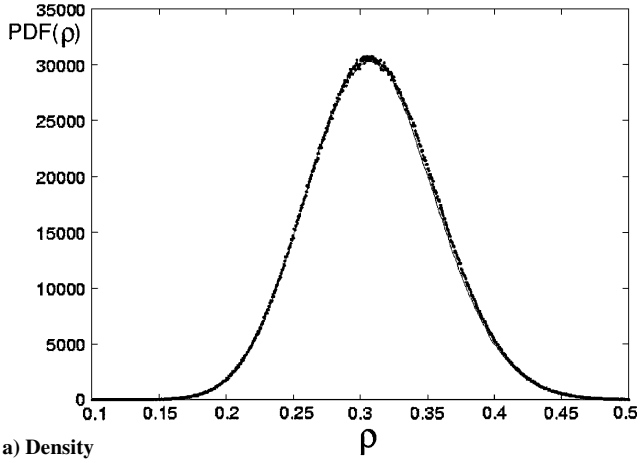

a) Density

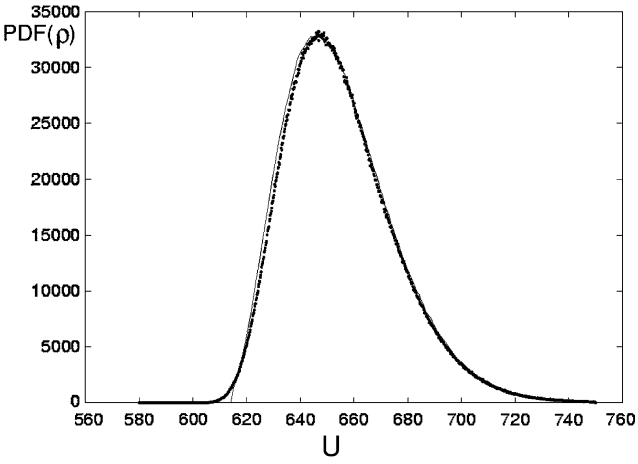

b) Velocity

Fig. 5 Nozzle outlet PDF (not normalized) for pressure and fluid velocity, one-dimensional, second order: ——, PC vs . . . . , MC.

Figure 5 shows the comparison between the PDFs obtained from the MC and PC techniques for the density and velocity at the outlet of the nozzle. The density (and pressure) PDF remains approximately

Gaussian at the nozzle exit, whereas the velocity PDF becomes skewed due to nonlinearity in the Euler equations. It can be seen that an excellent agreement between the two techniques is achieved, especially for the pressure where the two curves almost match. For the velocity, the agreement is very good except in the left tail region, indicating the need for higher order in the PC expansion to improve the approximation. Indeed, the MC PDF remains smooth for lower values of u, whereas the PC PDF shows a sharp stiff left tail. Meanwhile, this example clearly demonstrates the ability of the PC technique to propagate accurately uncertainty throughout the flow, even with a very limited number of terms in the expansion (three terms in this case). Considering the difference in the CPU time required (1.7×10^6 s for MC and 70 s for PC), the speed-up ratio is approximately 24,000, hence making the PC a much more effective alternative to the MC technique for this case. The cost of a single inviscid computation using one-dimensional, second-order PC takes roughly 13 times longer than a single inviscid, deterministic solution.

Two-Dimensional Stochastic Simulations

When the random variables of the problem considered are decoupled or, at most, only partially correlated, the stochastic process must be described using several independent random variables ξ. To illustrate this more general problem, a two-dimensional, second-order PC inviscid simulation is reported in this section. The inlet pressure and velocity are both assumed uncertain with no correlation while the inlet density is considered to be deterministic. Inlet pressure uncertainty is spanned along the stochastic dimension ξ_1 while velocity uncertainty is spanned along dimension ξ_2. The nozzle shape A is assumed uncertain as well and is expanded in a two-dimensional Karhunen–Loeve series. All variables are now expanded in six terms within the stochastic space.

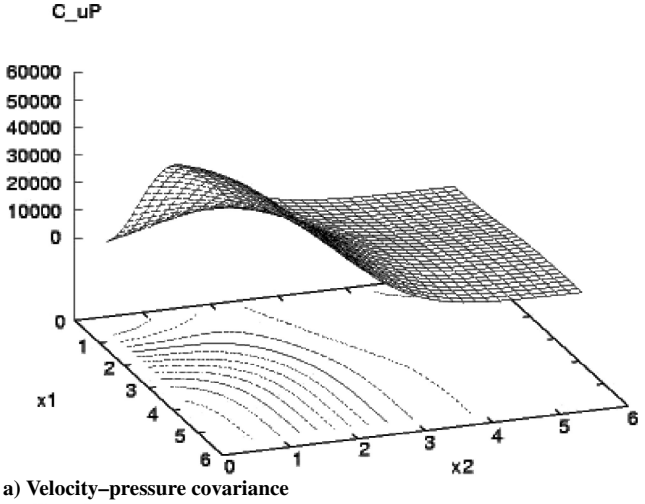

a) Velocity–pressure covariance

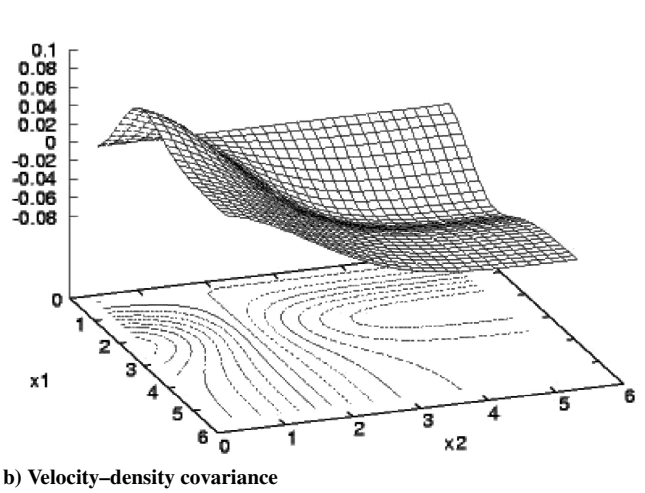

b) Velocity–density covariance

Fig. 6 Distribution of the covariance field throughout the nozzle.

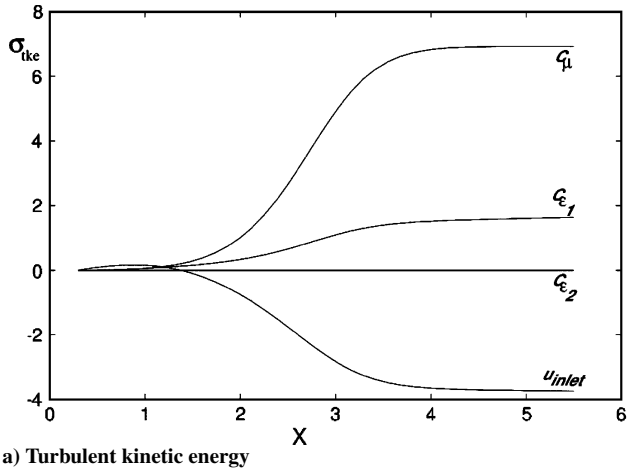

a) Turbulent kinetic energy

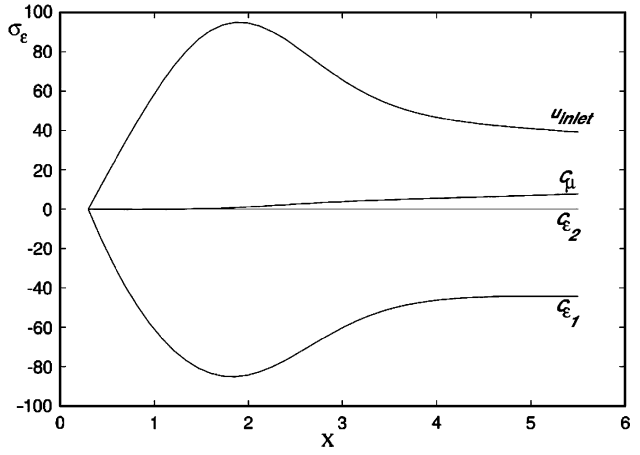

b) Turbulent dissipation rate

Fig. 7 Distribution of the deviation of the turbulence quantities along the nozzle due to uncertainty in different variables.

In Fig. 6, the covariance distribution is plotted for $u - P$ and $u - \rho$. Because all variables are set independent at the inlet, the covariance is zero at that point for all combinations. Downstream, coupling effects spread the uncertainty across the different variables, and the covariance evolves toward a steady state near the outlet of the nozzle.

Turbulence Simulation

Four separate viscous, turbulent cases have been run. In each case the PC is one-dimensional, second order. In each case the relevant variable is assumed Gaussian: 1) the inlet velocity u_{inlet} has a mean value of 450 $\text{m} \cdot \text{s}^{-1}$ with a 10 $\text{m} \cdot \text{s}^{-1}$ standard deviation, 2) the coefficient C_μ has a mean of 0.09 with a 10% standard deviation (=0.009), 3) the coefficient C_{ϵ_1} has a mean of 1.44 with a 0.1 standard deviation, and 4) the coefficient C_{ϵ_2} has a mean of 1.92 with a 0.1 standard deviation.

The effects of these uncertainties on the mean values of ρ, u, and P are negligible. A more noticeable effect is on the deviation of the turbulent flow variables k and ϵ from their deterministic values. These are shown in Fig. 7. The inlet velocity uncertainty affects the turbulent kinetic energy and the turbulent dissipation rate to about the same extent. The uncertainty in the modeling parameter C_{ϵ_1} has its greatest effect on the turbulent dissipation rate, whereas the parameter C_μ has a strong effect on the turbulent kinetic energy. The uncertainty in the modeling parameter C_{ϵ_2} has a much smaller effect than the uncertainties in the other three quantities.

Conclusions

In this paper, a PC approach, together with a spectral element method, was used to simulate the supersonic flow through a diverging nozzle in a quasi-one-dimensional approximation and to propagate the uncertainty thoughout the entire numerical field. Comparison with an MC simulation demonstrated its potential in terms of

ability and accuracy. However, this method performs poorly with high nonlinearities and cannot easily handle certain forms of equations (involving geometric or hypergeometric terms, for example) and other methods, such as the stochastic collocation method,[39,40] may be more suitable for thoses cases.

Appendix: Spectral and Stochastic Expressions for Inner Products and the k–ϵ Model

The equations to follow give the full Galerkin PC expressions for ν_t, k, and ϵ, and a representative scalar product in the spectral space. In the stochastic space, we have for a two-dimensional PC, for example,

$$\langle \Psi_a \Psi_b \Psi_c \Psi_d \Psi_e \rangle = \frac{1}{\sqrt{(2\pi)^2}} \int_{-\infty}^{\infty} \int_{-\infty}^{\infty} \Psi_a \Psi_b \Psi_c \Psi_d \Psi_e \, e^{-\frac{1}{2}\xi^T \xi} \, \mathrm{d}\boldsymbol{\xi} \tag{A1}$$

Typical inner product:

$$\begin{aligned}\left(h_i, \frac{\partial h_j}{\partial \bar{x}}, \frac{\partial h_l}{\partial \bar{x}}, h_m, h_k\right) &= \int_{-1}^{1} h_i(\bar{x}) \frac{\partial h_j}{\partial \bar{x}}, \frac{\partial h_l}{\partial \bar{x}} h_m(\bar{x}) h_k(\bar{x}) \, \mathrm{d}\bar{x} \\ &= \frac{32}{N^5} \sum_{a=0}^{N} \sum_{b=0}^{N} \sum_{c=0}^{N} \sum_{d=0}^{N} \sum_{e=0}^{N} \frac{T_a(\bar{x}_i) T_b(\bar{x}_j) T_c(\bar{x}_l) T_d(\bar{x}_m) T_e(\bar{x}_k)}{\bar{c}_a \bar{c}_b \bar{c}_c \bar{c}_d \bar{c}_e \bar{c}_i \bar{c}_j \bar{c}_l \bar{c}_m \bar{c}_k} \\ &\quad \times \int_{-1}^{1} T_a(\bar{x}) \frac{\partial T_b(\bar{x})}{\partial \bar{x}} \frac{\partial T_c(\bar{x})}{\partial \bar{x}} T_d(\bar{x}) T_e(\bar{x}) \, \mathrm{d}\bar{x}\end{aligned} \tag{A2}$$

The $\boldsymbol{\nu_t}$ expression is

$$\begin{aligned}&\sum_{i=0}^{N} \sum_{j=0}^{N} \sum_{a=0}^{N\mathrm{pc}} \sum_{b=0}^{N\mathrm{pc}} \nu_{i,a} \epsilon_{j,b} \langle \Psi_a \Psi_b \Psi_p \rangle (h_i, h_j, h_k) \\ &\quad = \sum_{i=0}^{N} \sum_{j=0}^{N} \sum_{a=0}^{N\mathrm{pc}} \sum_{b=0}^{N\mathrm{pc}} \sum_{c=0}^{N\mathrm{pc}} C_{\mu_c} k_{i,a} k_{j,b} \langle \Psi_a \Psi_b \Psi_c \Psi_p \rangle (h_i, h_j, h_k)\end{aligned} \tag{A3}$$

The $\boldsymbol{k}$ expression is

$$\begin{aligned}&\sum_{i=0}^{N} \sum_{j=0}^{N} \sum_{l=0}^{N} \sum_{a=0}^{N\mathrm{pc}} \sum_{b=0}^{N\mathrm{pc}} \sum_{c=0}^{N\mathrm{pc}} \sum_{d=0}^{N\mathrm{pc}} \rho_{i,a} U_{j,b} k_{l,c} \langle \Psi_a \Psi_b \Psi_c \Psi_d \Psi_p \rangle \\ &\quad \times \left\{ A_d \left[\left(\frac{\partial h_i}{\partial \bar{x}}, h_j, h_l, h_k \right) + \left(h_i, \frac{\partial h_j}{\partial \bar{x}}, h_l, h_k \right) \right.\right. \\ &\quad \left.\left. + \left(h_i, h_j, \frac{\partial h_l}{\partial \bar{x}}, h_k \right) \right] + \frac{\partial A_d}{\partial x} (h_i, h_j, h_l, h_k) \right\} \\ &\quad - (-1) \sum_{i=0}^{N} \sum_{j=0}^{N} \sum_{l=0}^{N} \sum_{a=0}^{N\mathrm{pc}} \sum_{b=0}^{N\mathrm{pc}} \sum_{c=0}^{N\mathrm{pc}} \sum_{d=0}^{N\mathrm{pc}} \rho_{i,a} \nu_{j,b} k_{l,c} A_d \\ &\quad \times \langle \Psi_a \Psi_b \Psi_c \Psi_d \Psi_p \rangle \left(h_i, h_j, \frac{\partial h_l}{\partial \bar{x}}, \frac{\partial h_k}{\partial \bar{x}} \right) \\ &\quad = 2 \sum_{i=0}^{N} \sum_{j=0}^{N} \sum_{l=0}^{N} \sum_{m=0}^{N} \sum_{a=0}^{N\mathrm{pc}} \sum_{b=0}^{N\mathrm{pc}} \sum_{c=0}^{N\mathrm{pc}} \sum_{d=0}^{N\mathrm{pc}} \sum_{e=0}^{N\mathrm{pc}} \rho_{i,a} \nu_{j,b} U_{l,c} U_{m,d} A_e \\ &\quad \times \langle \Psi_a \Psi_b \Psi_c \Psi_d \Psi_e \Psi_p \rangle \left(h_i, h_j, \frac{\partial h_l}{\partial \bar{x}}, \frac{\partial h_m}{\partial \bar{x}}, h_k \right) \\ &\quad - \sum_{i=0}^{N} \sum_{j=0}^{N} \sum_{a=0}^{N\mathrm{pc}} \sum_{b=0}^{N\mathrm{pc}} \sum_{c=0}^{N\mathrm{pc}} \rho_{i,a} \epsilon_{j,b} A_c \langle \Psi_a \Psi_b \Psi_c \Psi_p \rangle (h_i, h_j, h_k)\end{aligned} \tag{A4}$$

The $\boldsymbol{\epsilon}$ expression is

$$\begin{aligned}&\sum_{i=0}^{N} \sum_{j=0}^{N} \sum_{l=0}^{N} \sum_{m=0}^{N} \sum_{a=0}^{N\mathrm{pc}} \sum_{b=0}^{N\mathrm{pc}} \sum_{c=0}^{N\mathrm{pc}} \sum_{d=0}^{N\mathrm{pc}} \sum_{d=0}^{N\mathrm{pc}} \rho_{i,a} U_{j,b} k_{l,c} \epsilon_{m,d} \\ &\quad \times \langle \Psi_a \Psi_b \Psi_c \Psi_d \Psi_e \Psi_p \rangle \left\{ A_e \left[\left(\frac{\partial h_i}{\partial \bar{x}}, h_j, h_l, h_m, h_k \right) \right.\right. \\ &\quad \left. + \left(h_i, \frac{\partial h_j}{\partial \bar{x}}, h_l, h_m, h_k \right) + \left(h_i, h_j, h_l, \frac{\partial h_m}{\partial \bar{x}}, h_k \right) \right] \\ &\quad \left. + \frac{\partial A_e}{\partial x} (h_i, h_j, h_l, h_m, h_k) \right\} - (-1) \\ &\quad \times \sum_{i=0}^{N} \sum_{j=0}^{N} \sum_{l=0}^{N} \sum_{m=0}^{N} \sum_{a=0}^{N\mathrm{pc}} \sum_{b=0}^{N\mathrm{pc}} \sum_{c=0}^{N\mathrm{pc}} \sum_{d=0}^{N\mathrm{pc}} \sum_{e=0}^{N\mathrm{pc}} \rho_{i,a} \nu_{j,b} k_{l,c} \epsilon_{m,d} A_e \\ &\quad \times \langle \Psi_a \Psi_b \Psi_c \Psi_d \Psi_e \Psi_p \rangle \left[\left(h_i, h_j, h_l, \frac{\partial h_m}{\partial \bar{x}}, \frac{\partial h_k}{\partial \bar{x}} \right) \right. \\ &\quad \left. + \left(h_i, h_j, \frac{\partial h_l}{\partial \bar{x}}, \frac{\partial h_m}{\partial \bar{x}}, h_k \right) \right] \\ &\quad = 2 \sum_{i=0}^{N} \sum_{j=0}^{N} \sum_{l=0}^{N} \sum_{m=0}^{N} \sum_{o=0}^{N} \sum_{a=0}^{N\mathrm{pc}} \sum_{b=0}^{N\mathrm{pc}} \sum_{c=0}^{N\mathrm{pc}} \sum_{d=0}^{N\mathrm{pc}} \sum_{e=0}^{N\mathrm{pc}} \sum_{f=0}^{N\mathrm{pc}} \sum_{g=0}^{N\mathrm{pc}} \\ &\quad \times C_{\epsilon_{1\,g}} \rho_{i,a} \nu_{j,b} U_{l,c} U_{m,d} \epsilon_{o,e} A_f \langle \Psi_a \Psi_b \Psi_c \Psi_d \Psi_e \Psi_f \Psi_g \Psi_p \rangle \\ &\quad \times \left(h_i, h_j, \frac{\partial h_l}{\partial \bar{x}}, \frac{\partial h_m}{\partial \bar{x}}, h_o, h_k \right) \\ &\quad - \sum_{i=0}^{N} \sum_{j=0}^{N} \sum_{l=0}^{N} \sum_{a=0}^{N\mathrm{pc}} \sum_{b=0}^{N\mathrm{pc}} \sum_{c=0}^{N\mathrm{pc}} \sum_{d=0}^{N\mathrm{pc}} \sum_{e=0}^{N\mathrm{pc}} C_{\epsilon_{2\,e}} \rho_{i,a} \epsilon_{j,b} \epsilon_{l,c} A_d \\ &\quad \times \langle \Psi_a \Psi_b \Psi_c \Psi_d \Psi_e \Psi_p \rangle (h_i, h_j, h_l, h_k)\end{aligned} \tag{A5}$$

References

[1] Mehta, U. B., "Some Aspects of Uncertainty in Computational Fluid Dynamics Results," *Journal of Fluids Engineering*, Vol. 113, 1991, pp. 538–543.

[2] Roache, P. J., *Verification and Validation in Computational Science and Engineering*, Hermosa, Albuquerque, NM, 1998.

[3] Coleman, H. W., and Stern, F., "Uncertainties and CFD Code Validation," *Journal of Fluids Engineering*, Vol. 119, 1997, pp. 795–803.

[4] Oberkampf, W. L., and Blottner, F. G., "Issues in Computational Fluid Dynamics Code Verification and Validation," *AIAA Journal*, Vol. 36, No. 5, 1998, pp. 687–695.

[5] *AIAA Guide for the Verification and Validation of Computational Fluid Dynamics Simulations*, AIAA Standards Series, AIAA G-077-1998, AIAA, Reston, VA, 1998.

[6] Hemsch, M. J., "Statistical Analysis of CFD Solutions from the Drag Prediction Workshop," *Journal of Aircraft*, Vol. 41, No. 1, 2004, pp. 95–103; also AIAA Paper 2002-0842, 2002.

[7] Cosner, R. R., "The Importance of Uncertainty Estimation in Computational Fluid Dynamics," AIAA Paper 2003-0406, Jan. 2003.

[8] Tinoco, E. N., and Bussoletti, J. E., "Minimizing CFD Uncertainty for Commercial Aircraft Applications," AIAA Paper 2003-0407, Jan. 2003.

[9] Roache, P. J., "Error Bars for CFD," AIAA Paper 2003-0408, Jan. 2003.

[10] Luckring, J. M., Hemsch, M. J., and Morrison, J. H., "Uncertainty in Computational Aerodynamics," AIAA Paper 2003-0409, Jan. 2003.

[11] Stern, F., Wilson, R., and Shao, J., "Statistical Approach to CFD Code Certification," AIAA Paper 2003-0410, Jan. 2003.

[12] Mendenhall, M. R., Childs, R. E., and Morrison, J. H., "Best Practices for Reduction of Uncertainty in CFD Results," AIAA Paper 2003-0411, Jan. 2003.

[13] Pelletier, D., "Uncertainty Analysis by the Sensitivity Equation Method," AIAA Paper 2003-0412, Jan. 2003.

[14]Walters, R. W., "Towards Stochastic Fluid Mechanics via Polynomial Chaos," AIAA Paper 2003-0413, Jan. 2003.

[15]Freitas, C. J., Ghia, U., Celik, I., Roache, P., and Raad, P., "ASME's Quest to Quantify Numerical Uncertainty," AIAA Paper 2003-0627, Jan. 2003.

[16]Celik, I., Hu, G., and Badeau, A., "Further Refinement and Bench Marking of a Single-Grid Error Estimation Technique," AIAA Paper 2003-0628, Jan. 2003.

[17]Roy, C. J., and Hopkins, M. M., "Discretization Error Estimates Using Exact Solutions to Nearby Problems," AIAA Paper 2003-0629, Jan. 2003.

[18]Hanson, K. M., and Hemez, F. M., "Uncertainty Quantification of Simulation Codes Based on Experimental Data," AIAA Paper 2003-0630, Jan. 2003.

[19]Logan, R. W., and Nitta, C. K., "Validation, Uncertainty, and Quantitative Reliability at Confidence," AIAA Paper 2003-1337, Jan. 2003.

[20]Oberkampf, W. L., Diegert, K. V., Alvin, K. F., and Rutherford, B. M., "Variability, Uncertainty, and Error in Computational Simulation," *AIAA/ASME Joint Thermophysics and Heat Transfer Conference*, ASME-HTD-Vol. 357-2, American Society of Mechanical Engineers, 1998, pp. 259–272.

[21]Oberkampf, W. L., and Trucano, T. G., "Verification and Validation in Computational Fluid Dynamics," *Progress in Aerospace Sciences*, Vol. 38, No. 3, 2002, pp. 209–272.

[22]Walters, R. W., and Huyse, L., "Uncertainty Analysis for Fluid Mechanics with Applications," ICASE Rept. 2002-1, Feb. 2002; also available at URL: http://techreports.larc.nasa.gov/ltrs.

[23]Zang, T. A., Hemsch, M. J., Hilburger, M. W., Kenny, S. P., Luckring, J. M., Maghami, P., Padula, S. L., and Stroud, W. J., "Needs and Opportunities for Uncertainty-Based Multidisciplinary Design Methods for Aerospace Vehicles," NASA/TM-2002-211462, July 2002; also available at URL: http://techreports.larc.nasa.gov/ltrs.

[24]Oberkampf, W. L., Helton, J. C., and Sentz, K., "Mathematical Representation of Uncertainty," AIAA Paper 2001-1645, April 2001.

[25]Cao, Y., Hussaini, M. Y., and Zang, T. A., "Exploitation of Sensitivity Derivatives for Improving Sampling Methods," *AIAA Journal*, Vol. 42, No. 4, 2004, pp. 815–822; also AIAA Paper 2003-1656, April 2003; also available at URL: http://techreports.larc.nasa.gov/ltrs.

[26]Taylor, A. C., Green, L. L., Newman, P. A., and Putko, M. M., "Some Advanced Concepts in Discrete Aerodynamic Sensitivity Analysis," AIAA Paper 2001-2529, June 2001; also available at URL: http://techreports.larc.nasa.gov/ltrs.

[27]Le Maître, O. P., Knio, O. M., Najm, H. N., and Ghanem, R. G., "A Stochastic Projection for Fluid Flow. I—Basic Formulation," *Journal of Computational Physics*, Vol. 173, 2001, pp. 481–511.

[28]Le Maître, O. P., Reagan, M. T., Najm, H. N., Ghanem, R. G., and Knio, O. M., "A Stochastic Projection for Fluid Flow. II—Random Process," *Journal of Computational Physics*, Vol. 181, 2002, pp. 9–44.

[29]Xiu, D., Lucor, D., Su, S. H., and Karniadakis, G. E., "Stochastic Modeling of Flow–Structure Interactions Using Generalized Polynomial Chaos," *Journal of Fluids Engineering*, Vol. 124, No. 1, 2002, pp. 51–59.

[30]Xiu, D., and Karniadakis, G. E., "The Wiener–Askey Polynomial Chaos for Stochastic Differential Equations," *Journal on Scientific Computing*, Vol. 24, No. 2, 2002, pp. 619–644.

[31]Xiu, D., and Karniadakis, G. E., "Modeling Uncertainty in Flow Simulations via Generalized Polynomial Chaos," *Journal of Computational Physics*, Vol. 187, No. 1, 2003, pp. 137–167.

[32]Wiener, N., "The Homogeneous Chaos," *American Journal of Mathematics*, Vol. 60, 1938, pp. 897–936.

[33]Ghanem, R. G., and Spanos, P. D., *Stochastic Finite Elements: A Spectral Approach*, Springer-Verlag, New York, 1991.

[34]Ghanem, R., "Ingredients for a General Purpose Stochastic Finite Elements Implementation," *Computer Methods in Applied Mechanics and Engineering*, Vol. 168, 1999, pp. 19–34.

[35]Debusschere, B. J., Najm, H. N., Matta, A., Knio, O. M., Ghanem, R. G., and Le Maître, O. P., "Protein Labeling Reactions in Electrochemical Microchannel Flow: Numerical Simulation and Uncertainty Propagation," *Physics of Fluids*, Vol. 15, No. 8, 2003, pp. 2238–2250.

[36]Dunford, N., and Schwartz, J. T., *Linear Operator Theory*, Pt. 1, Wiley, New York, 1957, Chap. 4.

[37]Cameron, R. H., and Martin, W. T., "The Orthogonal Development of Nonlinear Functionals in Series of Fourier–Hermite Functionals," *Annals of Mathematics*, Vol. 48, 1947, pp. 385–392.

[38]Mathelin, L., and Hussaini, M. Y., "Uncertainty Quantification in CFD Simulations: A Stochastic Spectral Approach," *2nd International Conference on Computational Fluid Dynamics*, Springer-Verlag, 2003.

[39]Mathelin, L., Hussaini, M. Y., and Zang, T. A., "Stochastic Approaches to Uncertainty Quantification in CFD Simulations," *Numerical Algorithms* (to be published).

[40]Mathelin, L., and Hussaini, M. Y., "A Stochastic Collocation Algorithm for Uncertainty Analysis," NASA CR-2003-212153, Feb. 2003; also available online at URL: http://techreports.larc.nasa.gov/ltrs.

P. Givi
Associate Editor